

SliceLens: Fine-Grained and Grounded Error Slice Discovery for Multi-Instance Vision Tasks

Wei Zhang*, Chaoqun Wang*, Zixuan Guan, Sam Kao, Pengfei Zhao, Peng Wu, Sifeng He[†]
Apple

{wzhang52, chaoqun_wang, he_sifeng}@apple.com

Abstract

Systematic failures of computer vision models on subsets with coherent visual patterns, known as error slices, pose a critical challenge for robust model evaluation. Existing slice discovery methods are primarily developed for image classification, limiting their applicability to multi-instance tasks such as detection, segmentation, and pose estimation. In real-world scenarios, error slices often arise from corner cases involving complex visual relationships, where existing instance-level approaches lacking fine-grained reasoning struggle to yield meaningful insights. Moreover, current benchmarks are typically tailored to specific algorithms or biased toward image classification, with artificial ground truth that fails to reflect real model failures. To address these limitations, we propose **SliceLens**, a hypothesis-driven framework that leverages LLMs and VLMs to generate and verify diverse failure hypotheses through grounded visual reasoning, enabling reliable identification of fine-grained and interpretable error slices. We further introduce **FeSD** (Fine-grained Slice Discovery), the first benchmark specifically designed for evaluating fine-grained error slice discovery across instance-level vision tasks, featuring expert-annotated and carefully refined ground-truth slices with precise grounding to local error regions. Extensive experiments on both existing benchmarks and FeSD demonstrate that SliceLens achieves state-of-the-art performance, improving *Precision@10* by 0.42 (0.73 vs. 0.31) on FeSD, and identifies interpretable slices that facilitate actionable model improvements, as validated through model repair experiments.

1. Introduction

Despite the impressive performance of deep vision models, their reliability in real-world applications remains a concern due to systematic failures on specific subsets of data, known

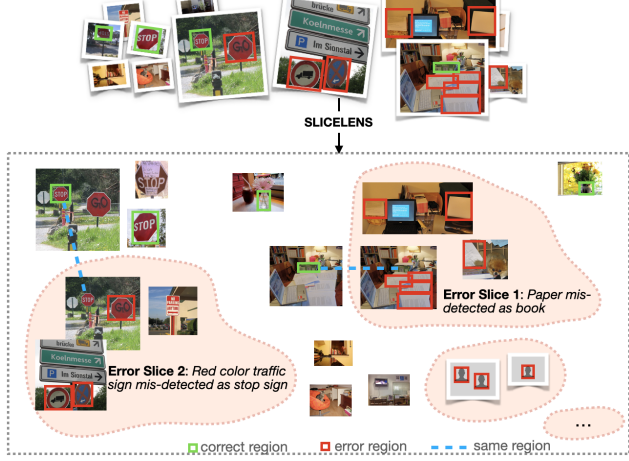


Figure 1. Error slice discovery illustrated on multi-instance tasks (e.g., detection).

as error slices [6]. These slices are characterized by coherent visual patterns that cause consistent mispredictions, revealing limitations in model robustness and generalization. Identifying and understanding these underperforming slices is crucial for building more trustworthy AI systems, particularly in high-stakes domains such as medical diagnosis [28, 32], autonomous driving [3], and robotics [39].

However, many existing slice discovery methods are primarily designed for image-level tasks such as classification [5, 9, 10, 12, 13, 37]. These approaches typically rely on clustering whole-image features [37], using image-level metadata [5, 10], or applying Large Language Model (LLM) reasoning to get image attributes [12]. Consequently, they are less effective for complex, multi-instance tasks like object detection or segmentation, where errors are often tied to fine-grained, instance-level attributes and their contextual relationships, as shown in Figure 1. Such crucial details can be obscured or lost when using whole-image representations.

Recent work has begun to address instance-level slice discovery [6, 36]. One method [36] clusters embeddings

*These authors contributed equally to this research.

[†]Corresponding Author, Project Lead

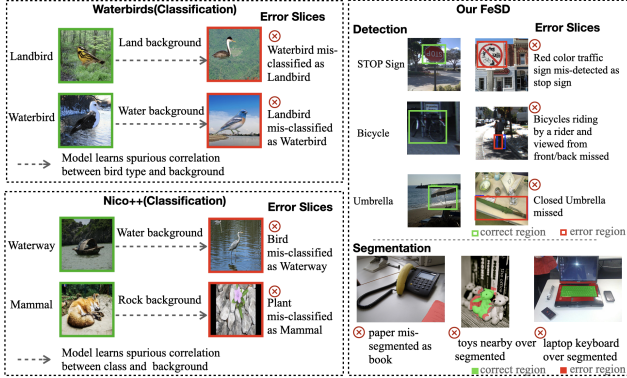


Figure 2. Comparison of error slice benchmark datasets.

from object patches and then uses an LLM to summarize the errors within each cluster. This bottom-up approach can be unreliable, as the initial visual clusters may lack a coherent semantic basis related to the errors. Another method [6], uses a Vision-Language Model (VLM) to generate descriptive tags for each object instance, making the identification of coherent slices from large quantity of tag combinations difficult. The complex failure modes with compositional and relational concepts are not easily captured by local patch embeddings or represented by a conjunction of atomized tags, highlighting the need for a more direct reasoning with both grounding and context information.

Progress in error slice discovery is further hindered by the absence of adequate benchmarks. Current benchmarks are often limited to image classification and rely on spurious correlations [30, 38] which fails to represent the complexity of errors in tasks like object detection, as shown in the left column of Figure 2. Consequently, there is no standardized way to evaluate a method’s ability to find fine-grained, grounded error slices, making it difficult to quantitatively compare approaches and measure progress.

To address these gaps, we propose SliceLens, a method for discovering error slices through a hypothesis-driven framework that integrates fine-grained, grounded visual reasoning. It directly formulates and tests hypotheses about complex failure modes as holistic natural language descriptions, bypassing the limitations of tag-based approaches. To enable standardized evaluation, we present FeSD (Fine-grained Slice Discovery), a comprehensive benchmark with expert-annotated ground-truth slices that embody the fine-grained and compositional challenges of real-world model failures. Our main contributions are:

1. We propose SliceLens, a novel method that employs a hypothesis generate-and-verify paradigm for fine-grained and grounded error slice discovery. It uses both LLM and VLM to generate diverse hypotheses, which are then validated using the grounded reasoning capabilities of VLM. A final trend analysis, linking slice defini-

tion confidence to model error rates, ensures the discovery of highly reliable error slices.

2. We establish **FeSD** (Fine-grained Slice Discovery), the first benchmark specifically designed for evaluating fine-grained error slice discovery across instance-level vision tasks. The slices are created by experts and each data sample is labeled and refined by annotators, which contain fine-grained contextual interference, semantic confusion, and intrinsic visual difficulties with grounding information to local error regions.
3. Extensive experiments demonstrate the strong effectiveness and generalizability of SliceLens, achieving state-of-the-art performance for fine-grained slice discovery on FeSD, improving Precision@10 by an absolute 0.42 (0.73 vs. 0.31). Model repair experiments validate its practicality, showing model performance improvement across both classification and detection tasks.

2. Related Work

2.1. Slice Discovery Methods

Existing error slice discovery methods can be broadly classified by their operational granularity into two main categories: image-level approaches, which typically focus on classification tasks, and instance-level approaches, which address fine-grained challenges in tasks like object detection.

Image level slice discovery methods. Early automated methods depend on clustering or fitting models on extracted embeddings [7, 9, 34, 37]. For example, FD (Feature Discovery) [16] discovers error slices by analyzing and clustering feature representations. Domino [9] leverages cross-modal embeddings to discover systematic errors by projecting visual features into a shared multimodal space and identifying failure modes through mixture modeling. FACTS [37] employs a two-stage approach: first amplifying spurious correlations through strongly regularized training, then performing correlation-aware slicing via mixture modeling in bias-aligned feature space. A key limitation of this paradigm is interpretability, as the discovered slices in embedding spaces are often hard to understand. To improve interpretability, recent work has shifted to a “tag-then-slice” approach. These methods first generate a discrete set of semantic attributes and then search for data matching these attributes or their combinations associated with poor model performance [5, 6, 13, 25]. HiBug [5] using LLMs to propose attributes or tags, followed by algorithms to navigate the combinatorial space. B2T (Bias-to-Text) [17] extracts keywords from captions of misclassified samples and validates them with VLM similarity, enabling the discovery and naming of contextual biases such as background bias in Waterbirds. LADDER [12] leverages LLMs to induce systematic biases from model activations and metadata, producing

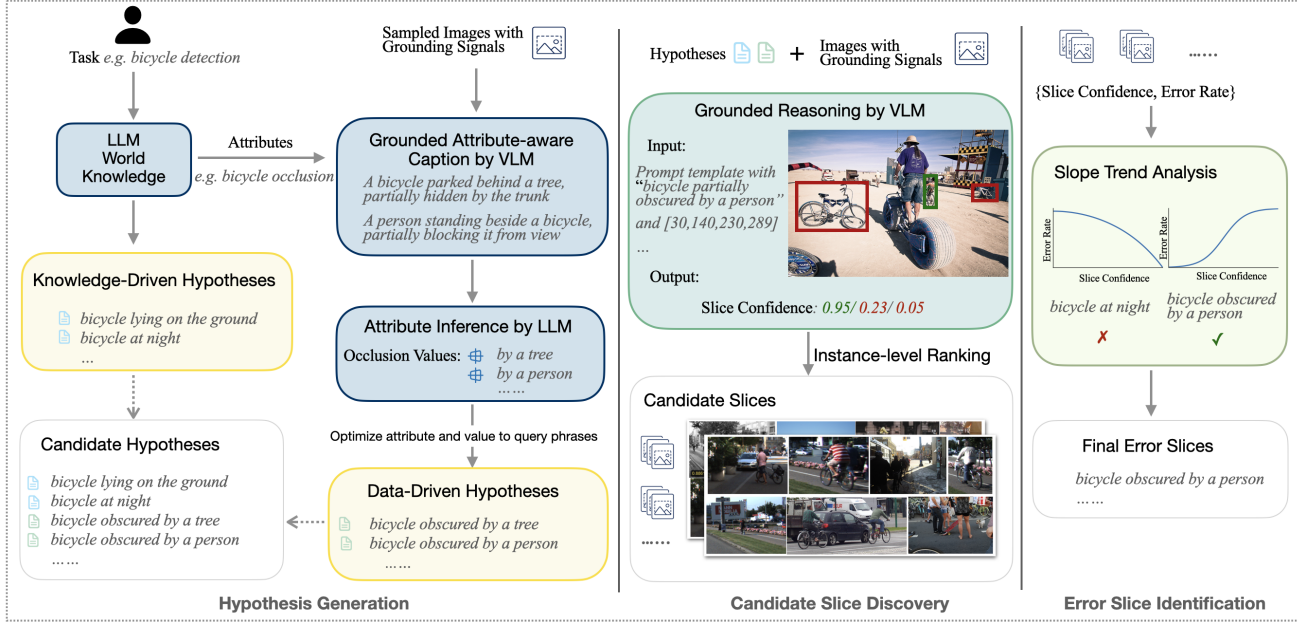


Figure 3. Overview of SliceLens. Illustrated with the “bicycle detection” example.

testable hypotheses and pseudo-labels for error correction. ViG-Bias [27] extends FACTS to ViG-FACTS with vision-language grounding, incorporating textual descriptions to improve slice discovery accuracy and interpretability, the same with B2T extended to ViG-B2T.

Instance level slice discovery methods. VISLIX [36] is an interactive platform for object detection failure analysis, employing a bottom-up “cluster-then-explain” strategy. It first clusters embeddings from object patches, uses an LLM to describe errors for each data by predefined questions and then summarize the errors. These text descriptions are for human verification interactively. An alternative direction, proposed by HiBug2 [6], uses a VLM to generate descriptive tags for each object instance. However, the underlying “bag-of-tags” mechanism struggles to scale to complex scenarios. The combinatorial explosion of tags makes the search for meaningful error patterns computationally challenging and prone to discovering spurious correlations.

Our SliceLens method complements prior approaches by explicitly introducing fine-grained, grounded visual patterns as the hypothesis space, and by performing a generate-verify step based on visual reasoning to discover interpretable slices across tasks.

2.2. Benchmark Datasets for Error Slice Discovery

Slice-oriented benchmark for classification task. While widely used for fairness and bias research, prominent datasets like [24, 30, 38] have limitations for capturing real-world failure modes. For instance, Waterbirds [30] is known for its artificial cut-and-paste construction which

induces overly strong background correlations [23, 35]. CelebA [24] suffers from severe attribute imbalances and hidden correlations that complicate fairness evaluations [1, 31]. Similarly, NICO++ [38] has been noted for its narrow and ambiguous contextual domains [15]. Collectively, these benchmarks rely on simplified spurious correlations and artificial contexts, restricting them to classification tasks and failing to represent complex real-world challenges such as occlusion, scale variation, and cluttered backgrounds.

OOD(Out Of Distribution) benchmark for complex task. Benchmarks targeting OOD have also emerged in detection and segmentation. In object detection, COCO-O [26] introduces natural distribution shifts. In segmentation, benchmarks such as Fishscapes [3] focus on synthetic anomalies, while medical segmentation benchmark [19] emphasizing failure detection under distribution shift with risk-coverage analysis. However, their goal is to evaluate OOD generalization, not to provide the interpretable, fine-grained ground-truth slices required for root cause analysis of failures.

Existing slice benchmarks [24, 30, 38] lack support for instance-level tasks. OOD benchmarks reveal systematic errors but do not provide slice-level interpretability or fine-grained ground truth. Our FeSD benchmark is designed to fill this gap, providing fine-grained and interpretable slice annotations across detection and segmentation tasks.

3. SliceLens for Fine-grained Slice Discovery

The proposed SliceLens method consists of two key modules: hypothesis generation and hypothesis verification. The generation module leverages both world knowledge and data-driven analysis to formulate hypotheses, while the verification module uses grounded VLM reasoning to statistically validate them as systematic errors. To explain the workflow more clearly, an example of discovering the error slice “bicycle obscured by a person” for bicycle detection is illustrated in Figure 3.

3.1. Error Slice Hypothesis Generation

To comprehensively cover different types of model failures, our hypothesis generation module operates in two complementary modes, inspired by the categorization of errors into inherent task difficulties and data distribution issues [6].

1. Knowledge-Driven Hypothesis Generation. To capture inherent task difficulties, SliceLens leverages LLM using a brief task context in a top-down way (prompt in Appendix Figure 8). Leveraging broad world knowledge on the task, the LLM proposes reasonable failure cases that often align closely with real error modes, such as “background objects similar to bicycles” or “very small objects” for object detection tasks.

2. Data-Driven Hypothesis Generation. To uncover errors arising from distributional issues specific to the dataset, SliceLens performs a data-driven analysis in a bottom-up way. Based on semantic attributes observed in the data, the hypotheses are generated in three steps (prompt templates in Appendix Figure 9, Figure 10 and Figure 11): (a) *Grounded Attribute-aware Caption Extraction*: The knowledge-driven hypotheses also consist of attributes associated with task failures. For each image from a sampled subset, a VLM is employed to generate attribute-aware textual captions that are explicitly grounded to specific objects or regions. (b) *Attribute Inference*: An LLM then processes these captions to infer a diverse set of potential semantic attribute values. This is similar to text-conditional clustering methods like TCIC [20], but it differs by not relying on image-level captions. (c) *Hypothesis Generation*: Finally, the attributes and values are optimized by an LLM into well-formed query phrases in natural language that serve as concrete, data-driven hypotheses to be tested in the verification stage.

Given the task “bicycle detection”, SliceLens generates: (1) knowledge-driven hypotheses, which capture inherent difficulties such as detecting “bicycle lying on the ground” or “bicycle at night”; and (2) data-driven hypotheses with LLM-generated abstract attributes like “bicycle occlusion”, which are then inferred by a VLM into fine-grained, visually grounded values such as “by a car” or “by a person”. Finally, the attributes and values are optimized into natural language as “bicycle obscured by a car” and “bicycle ob-

scured by a person”.

3.2. Error Slices Verification

Given a set of hypotheses, SliceLens retrieves the data instances that satisfy each hypothesis, thereby discovering candidate slices. It then performs error verification to determine whether these slices correspond to systematic model failures.

3.2.1. Grounded Candidate Slices Discovery

Metadata or tags can hardly describe visual slices specific to an instance or object with complex object relationships and multiple composed logic conditions, which are likely appear in real model deployment scenarios. To support complex hypothesis as query, we leverage the grounding and visual reasoning capabilities of VLM. Given an image I and a query phrase q , our goal is to determine whether an error region $r \subset I$ in I satisfies the query. The error regions are from false negatives or false positives of detection and segmentation tasks. We ground error regions with bounding boxes for detection, whereas for segmentation, we can use bounding boxes of masks or points in regions.

Point-based prompt template: “If the region pointed to by point_2d: (x, y) matches the description q , please answer yes else no.” where (x, y) denotes the 2D coordinate within the error region.

Bounding box-based prompt template: “If the region $[x_{\min}, y_{\min}, x_{\max}, y_{\max}]$ matches the description q , please answer yes else no.”

During inference, a VLM (e.g., Qwen2.5-VL [2]) compute the logits of the output “yes” token and the “no” token, based on a prompt that incorporates the hypothesis and grounding signals. Formally, the logit for token t is denoted as $z(t | \mathcal{P}(q, r))$. Applying softmax over the candidate tokens, we obtain:

$$P(\text{yes} | q, r) = \frac{\exp(z(\text{yes} | \mathcal{P}(q, r)))}{\exp(z(\text{yes} | \mathcal{P}(q, r))) + \exp(z(\text{no} | \mathcal{P}(q, r)))}. \quad (1)$$

The **slice confidence** for error region r is defined as $P(\text{yes} | q, r)$.

For the selected hypothesis “bicycle obscured by a person”, SliceLens retrieves relevant instances by ranking the slice confidence of all instances. The retrieved examples form a slice that illustrates various scenarios where bicycles are partially occluded by a person.

3.2.2. Automated Error Slice Identification

Existing approaches often ignore the accuracy of metadata or tag and identify error slices by thresholding slice error rates [6, 12], overlooking the reliability of slice data. SliceLens addresses this limitation by performing a dynamic **slope trend analysis**. It quantifies the statistical relationship between slice confidence and error rates: a slice is con-

sidered a systematic error region if the error likelihood increases monotonically with slice confidence. Specifically, a sliding threshold defines overlapping windows where confidence exceeds a given value, which selects relatively high confidence data. Within each window, a local linear fit is computed between selected data confidence and error rate, and the maximum positive slope is recorded. A slice is classified as a systematic error if this slope indicates a consistently increasing error trend. The method is robust to parameter settings, leading to more reliable and defensible model diagnosis.

For the “bicycle obscured by a person” slice, the trend analysis reveals a strong positive trend between slice confidence and actual error rates. As shown in Figure 3, instances with higher similarity to the “bicycle at night” hypothesis exhibit lower error rates, confirming this not a genuine error slice.

4. FeSD(Fine-grained Slice Discovery)Dataset

4.1. FeSD Dataset Construction

To address the limitations of existing benchmarks (see Section 2.2 and Figure 2), we constructed FeSD, a new benchmark dataset designed to capture realistic, fine-grained, and instance-level error slices. The FeSD dataset is built upon a combination of over 12,000 images from three widely used public validation sets: COCO (5k images)[21], KITTI (3,769 images)[11], and a public face detection set (3,347 images)[8]. We followed a four-step pipeline to identify and annotate error slices:

1. **Model Errors Collection:** We ran five representative object detectors (YOLO [33], Faster R-CNN [29], RetinaNet [22] and DETR [4]) and a segmentation model (Mask R-CNN [14]) on the combined validation images to gather a diverse set of predictions. With original ground truth annotations and model predictions, the model errors are computed and aggregated as insights for realistic failure patterns.
2. **Expert-Driven Slice Definition:** Based on failure patterns observed, domain experts defined and validated a comprehensive set of error slices, comprising 21 for detection and another 21 for segmentation, for a total of 42 distinct slices.
3. **Slice Discovery by Human Annotation:** This was the most labor-intensive step, requiring 1500 person-hours of annotation effort. For each of the error slices, annotators thoroughly reviewed every relevant instance to (a) verify that it belonged to the slice definition and exhibited the correct failure type, and (b) correct its bounding box and/or segmentation mask to ensure geometric accuracy.
4. **Dataset Refinement:** For all instances not belonging to any defined error slice, model predictions were overwrit-

ten by ground truth. This crucial step eliminates potential noise and ensures that the final dataset contains only clean, unambiguous annotations for non-slice instances.

4.2. FeSD Dataset Categories

The error slices in FeSD contain location and category errors, including both false negatives (FN) and false positives (FP). We provide error regions (FN or FP) with bounding boxes or segmentation masks, along with slice descriptions in the dataset. The error slices are organized into three primary categories: (1) Semantic Confusion, covering errors arising from the model’s conceptual understanding, including confusion where visually similar classes are mistaken for one another and errors on abstract or symbolic representations; (2) Contextual Interference, encompassing errors caused by an object’s surroundings or relationships, such as inter-object occlusion, spurious contextual biases, and part–whole confusion; and (3) Intrinsic Visual Difficulty, referring to failures caused by the inherent visual properties of the object instance itself, including degraded views, non-canonical viewpoints, and significant self-occlusion or partial views.

The error slices are derived from realistic instance-level inference errors and subsequently annotated by human experts to ensure quality. The complete set of error slices is provided in Appendix Table 8 and Table 7.

5. Experiments

We conduct comprehensive experiments to evaluate SliceLens against state-of-the-art error slice discovery methods. Our evaluation encompasses widely-used bias discovery benchmarks and our newly constructed fine-grained dataset, demonstrating the effectiveness and generalizability of our approach across diverse scenarios.

5.1. Evaluation on Bias Discovery Datasets

5.1.1. Experimental Setup

We compare SliceLens against seven state-of-the-art error slice discovery methods, including:(1) embedding based **FD** (Feature Discovery) [16], **Domino** [9], and **FACTS** [37](2) interpretability based **LADDER** [12],**ViG-FACTS** [27],**B2T** (Bias-to-Text) [17] and **ViG-B2T** [27](See Section 2.1 for more details).

We evaluate our method on three bias discovery benchmarks: (1) Waterbirds [30], which contains two error-prone slices used for bias evaluation: waterbirds on land and landbirds on water; (2) CelebA [24], where, following [37], we focus on the blonde hair classification task that exhibits a spurious correlation between gender and hair color (males with non-blonde hair, females with blonde hair); and(3)NICO++ [38], where we simulate controlled spurious-correlation settings following FACTS [37] and

evaluate under three correlation strengths—75%, 90%, and 95%—representing increasing levels of spurious association between concepts and contexts. We employ **Precision@k** as our primary evaluation metric following [9, 37]. This metric measures the precision of the top-k retrieved samples for each ground-truth error slice. Formally, for a ground truth slice S_{gt} and predicted slice S_{pred} , Precision@k is defined as:

$$\text{Precision@k} = \frac{|S_{gt} \cap S_{pred}^{(k)}|}{k} \quad (2)$$

where $S_{pred}^{(k)}$ represents the top-k samples in the candidate slice ranked by confidence scores. Following prior work, we set $k = 10$ for all experiments, or the actual size if the slice has fewer than 10 samples.

5.1.2. Implementation Details

To get predictions for model errors, for Waterbirds and CelebA experiments we utilize pre-trained model checkpoints provided by LADDER [12], which were trained with standard empirical risk minimization (ERM). For NICO++ experiments, we train models following the FACTS codes [37], using ResNet-50 with learning rate 10^{-5} and weight decay sweeping over $[10^{-3}, 10^{-2}, 10^{-1}, 1.0, 2.0]$ to amplify spurious correlations. We report the performance metrics directly from the original papers for all compared methods. For Ladder on NICO++, where results were not available, we generated them by running the FACTS training codes [37] and Ladder’s slice finding codes.

Our SliceLens implementation employs Gemini-2.5-Pro as LLM and Qwen-2.5-VL-7B as VLM, selected for a trade-off between performance and efficiency (ablation in Appendix B.1). Prompts of SliceLens are in Appendix A.1.

5.1.3. Results

Table 1. **Precision@10 results on bias discovery datasets.** Best results are shown in **bold**, second-best are underlined.

Method	Waterbirds	CelebA	NICO++(75/90/95)
FD	0.90	0.70	0.19/0.19/0.19
Domino	1.00	<u>0.90</u>	0.24/0.25/0.27
FACTS	1.00	<u>0.90</u>	0.56/0.60/0.62
LADDER	0.86	0.85	0.32/0.52/0.54
ViG-FACTS	1.00	1.00	<u>0.60/ 0.67/ 0.65</u>
B2T	0.92	0.64	-
ViG-B2T	<u>0.97</u>	0.70	-
SliceLens (Ours)	1.00	1.00	0.64/0.66/0.69

Table 1 presents the results across three classification benchmark datasets. On Waterbirds and CelebA, SliceLens achieves perfect Precision@10 scores of 1.0, matching the best performance of existing methods. The two datasets

contain relatively simple spurious correlations that can be effectively captured by various approaches.

The most significant improvements are observed on NICO++, which presents more complex spurious correlations. SliceLens achieves the best performance on two out of three correlation settings (75% and 95%), with relative improvements of 6.7% and 6.2% (over the previous best method ViG-FACTS, improving from 0.60 to 0.64 and 0.65 to 0.69, respectively). On the 90% setting, SliceLens achieves competitive second-best performance (0.66 vs. 0.67). This demonstrates the effectiveness of our approach in handling complex biases.

5.2. Evaluation on the FeSD Dataset

To evaluate performance on our FeSD dataset, we compare SliceLens against two recent open-source methods, FACTS and HiBug. As FACTS is an image-level method, we adapt it by aggregating instance errors to an image-level error rate. We adapt HiBug’s tagging mechanism from the image level to the object level to enable instance-based comparison.

The following evaluations focus on detection-based error slices in FeSD. Results on segmentation-based error slices are further reported in Appendix B.4.2. Detailed results are presented in Appendix Table 7 and Table 8, serving as baseline references for future studies.

Table 2. **Precision@10 results on FeSD dataset.** *Method adapted from image-level to instance-level evaluation.

Method	FACTS*	HiBug*	SliceLens
Precision@10	0.28	0.31	0.73

As shown in Table 2, SliceLens consistently outperforms both baseline methods across all error categories, achieving an average precision@10 of 0.73 compared to HiBug* (0.31) and FACTS* (0.28). This substantial improvement of 0.42 over the 0.31 baseline demonstrates the critical importance of spatial grounding and reasoning for fine-grained error slice discovery in detection tasks.

To demonstrate the robustness of SliceLens across diverse error slices, Figure 4 shows the precision@10 performance comparison broken down by categories from our slice taxonomy(Section 4.2). SliceLens demonstrates particularly strong performance on *Intrinsic Visual Difficulty* errors (0.76), while both baseline methods struggle with this challenging category, with HiBug* achieving only 0.19 and FACTS* achieving 0.16. The method also shows robust performance on *Semantic confusion* (0.71) and *Contextual interference* (0.70), highlighting the advantage of our adaptive hypothesis generation approach for comprehensive model debugging across diverse detection scenarios.

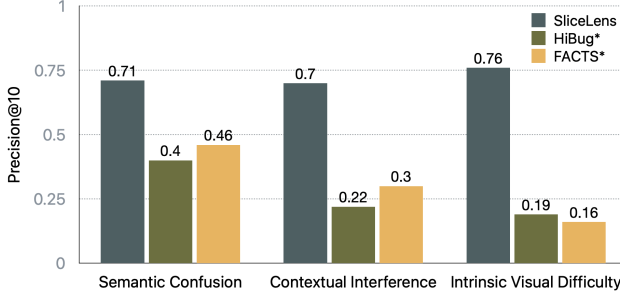


Figure 4. Performance comparison across different error categories.

5.3. Ablation Studies of SliceLens

5.3.1. Hypothesis Generation

We compare the proposed language-based hypotheses with attribute-based tags (HiBug*) in terms of their semantic alignment with the ground-truth failure slices, using results from Section 5.2. Specifically, an LLM-based (Gemini-2.5-pro) evaluator determines whether a discovered slice is semantically related to any ground-truth slice (prompt in Appendix A.3). A slice is considered correct if the evaluator judges it as relevant. *Recall* measures the proportion of ground-truth slices that are successfully retrieved, while *precision* measures the proportion of discovered slices that are semantically aligned with the ground truth. The language-based hypotheses containing 102 slices achieve a *recall* of 0.90 and *precision* of 0.74 when evaluated for semantic relevance to ground-truth error slices. In contrast, the attribute-based tagging method exhaustively enumerates 70 single-attribute, 2,083 dual-attribute, and 36,486 triple-attribute combinations, yielding 0.57 *recall* and 0.54 *precision* under a loose matching criterion. Figure 5 illustrates that language-based hypotheses capture the semantic structure of real-world failure patterns more coherently and compactly than attribute-based tags with better interpretability.

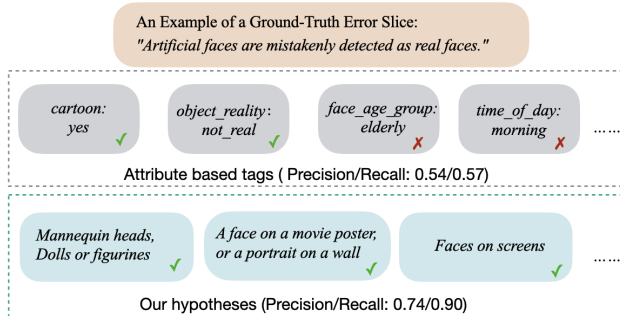


Figure 5. Comparison between tags and our hypotheses on semantic relevance with ground truth error slices.

5.3.2. Grounded Slice Discovery

A key innovation of SliceLens is instance-level analysis through spatial grounding, crucial for multi-object detection tasks. We compare this against image-level analysis on the “faces partially hidden by objects” slice from FeSD.

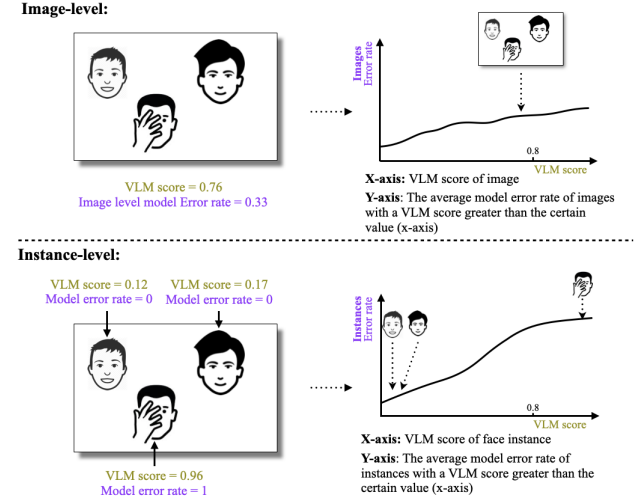


Figure 6. Why grounded (instance-level) retrieval reveals failure slices while image-level retrieval dilutes them. Instance-level retrieval produces stronger alignment between VLM similarity and model errors.

Figure 6 illustrates how instance-level analysis produces stronger alignment between VLM similarity and model errors compared to image-level analysis. Quantitatively, instance-level analysis achieves precision@10 of 0.80 versus 0.60 for image-level analysis. Our slope trend analysis reveals that the VLM score-accuracy curve has a slope of 1.32 for instance-level versus 0.84 for image-level. This superior performance stems from avoiding the dilution effect where failures of challenging instances are masked by correct predictions on other instances within the same image.

5.3.3. Automated Error Slice Identification

We evaluate how well the automatically identified error slices preserve the hypotheses that are semantically consistent with the ground-truth (GT) while filtering out inconsistent ones. Existing methods classify a slice as an error if its error rate exceeds average by a predefined threshold *error_threshold* [6, 12]. In contrast, our slope trend analysis method determines errors based on the slope of the local confidence-error relationship, where slices with slope greater than *slope_threshold* are identified as error. For all discovered slices, we compute the recall of GT-consistent hypotheses, the precision of identified error slices against GT and the *F1* score. As shown in Figure 7, the slope trend analysis method not only achieves a higher (3.7% on average) *F1* score compared to the error-rate thresholding base-

line, but also demonstrates greater robustness to threshold selection. This also indicates that our approach can effectively mitigate the confidence thresholding sensitivity commonly observed in slice discovery methods.

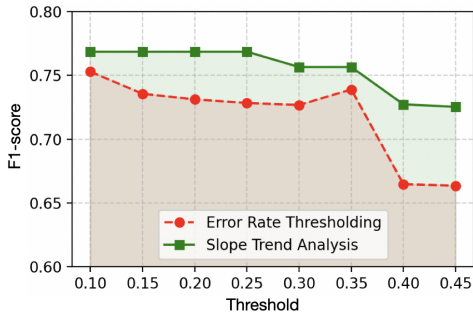


Figure 7. Comparison between error rate thresholding and slope trend analysis for error slice identification.

5.4. Model Improvement and Practical Impact

5.4.1. Model Improvement on Image Classification

We evaluate the actionability of discovered slices via a model repair experiment on the CelebA and Waterbirds datasets, following the setup from [12]. To ensure a fair comparison across methods with fundamentally different slice definition strategies, we employ two distinct repair protocols. For Ladder, which generates global slice definitions, we use its native procedure of fine-tuning a separate classifier per slice and ensembling their predictions. However, this approach is not applicable to Facts, Domino, and SliceLens, as they identify slices only within data subsets, making their outputs incompatible with Ladder’s ensembling logic. Therefore, for these methods, we adopt the unified Discriminative Fine-tuning for Repair (DFR) framework [18]. We compute a single failure score for each sample by taking the maximum similarity across all discovered slices and then fine-tune the classifier head on the subsets with the highest and lowest scores. Details can be found in Appendix B.3.1.

Table 3 shows that our method achieves comparable or slightly better results than all other slice discovery baselines, demonstrating the effectiveness of the discovered error slices in mitigating errors caused by spurious correlations in image classification.

5.4.2. Object Detection Model Improvement on Fine-Grained Patterns

In this experiment, we showed that SliceLens enables grounded model repair for object detection (e.g., bicycles). After identifying the error slice “bicycle partially occluded by a person” on FeSD, we obtain instance-level slice confidence scores using SliceLens slice discovery on the COCO

Table 3. **Worst Group Accuracy (WGA) results.** Best results are shown in **bold**, second-best are underlined. All results are averaged over 10 independent runs to account for the stochasticity of SGD during fine-tuning.

Method	Waterbirds	CelebA
Ladder	0.896 ± 0.014	0.878 ± 0.015
Domino	0.898 ± 0.022	0.827 ± 0.002
FACTS	0.889 ± 0.028	0.6 ± 0.011
SliceLens (Ours)	0.904 ± 0.017	0.882 ± 0.004

Table 4. Model repair performance on bicycle detection. Results are averaged over 3 repetitions.

Method	mAP-bicycle	mAR-bicycle
No model repair	27.2	39.33
Baseline model repair	28.58 ± 0.016	41.14 ± 0.031
GroupDRO + Slicelens	33.59 ± 0.028	47.09 ± 0.23

training dataset. As a baseline for the Faster R-CNN pre-trained model, we fine-tune it on all COCO training images containing at least one bicycle instance. For repair, we adapt the online GroupDRO framework [30] to instance level: each object class is treated as a group, and an image-level binary attribute is defined by thresholding the maximum instance-level slice confidence score at 0.9. This setup allows GroupDRO’s reweighting to focus specifically on images likely exhibiting the failure pattern, applied only to detection head losses (classification and box regression) during fine-tuning. Details can be found in Appendix B.3.2.

Table 4 shows that our model repair strategy substantially improves both the bicycle-class mAP and mAR. Our method leverages instance-level slice data for more targeted model adaptation, outperforming baseline repair approaches. This validates that the grounded discovery strategy in SliceLens is effective for repairing instance-level failure patterns in object detection.

6. Conclusion

We present **SliceLens**, a fine-grained error slice discovery method for multi-instance vision tasks. It adopts a hypothesis-driven approach that combines LLM- and VLM-based reasoning to generate and verify grounded hypotheses about model failures. We also introduce **FeSD**, a benchmark with expert-annotated, fine-grained slices and precise grounding. Experiments show that SliceLens effectively identifies complex, interpretable error patterns, offering actionable insights for model debugging. Despite its promise, assessing the completeness of hypothesis generation remains challenging in open-world settings. Future work will explore principled metrics for evaluating slice completeness in real-world applications.

References

[1] Mohsan Alvi, Andrew Zisserman, and Christoffer Nellåker. Turning a blind eye: Explicit removal of biases and variation from deep neural network embeddings. In *ECCV Workshop*, pages 0–0, 2018. 3

[2] Shuai Bai, Keqin Chen, Xuejing Liu, Jialin Wang, Wenbin Ge, Sibo Song, Kai Dang, Peng Wang, Shijie Wang, Jun Tang, Humen Zhong, Yuanzhi Zhu, Mingkun Yang, Zhao-hai Li, Jianqiang Wan, Pengfei Wang, Wei Ding, Zheren Fu, Yiheng Xu, Jiabo Ye, Xi Zhang, Tianbao Xie, Zesen Cheng, Hang Zhang, Zhibo Yang, Haiyang Xu, and Junyang Lin. Qwen2.5-vl technical report. *arXiv preprint arXiv:2502.13923*, 2025. 4

[3] Hermann Blum, Paul-Edouard Sarlin, Juan Nieto, Roland Siegwart, and Cesar Cadena. The fishscapes benchmark: Measuring blind spots in semantic segmentation. *IJCV*, 129(12):3119–3135, 2021. 1, 3

[4] Nicolas Carion, Francisco Massa, Gabriel Synnaeve, Nicolas Usunier, Alexander Kirillov, and Sergey Zagoruyko. End-to-end object detection with transformers. In *ECCV*, pages 213–229, 2020. 5

[5] Muxi Chen, Yu Li, and Qiang Xu. Hibug: On human-interpretable model debug. In *NeurIPS*, pages 4753–4766, 2023. 1, 2

[6] Muxi Chen, Chenchen Zhao, and Qiang Xu. Hibug2: Efficient and interpretable error slice discovery for comprehensive model debugging. In *ICLR*, 2025. 1, 2, 3, 4, 7

[7] Greg d’Eon, Jason d’Eon, James R. Wright, and Kevin Leyton-Brown. The spotlight: A general method for discovering systematic errors in deep learning models. In *Proceedings of the 2022 ACM Conference on Fairness, Accountability, and Transparency (FAccT)*, pages 1962–1981, 2022. 2

[8] Fares Elmenshawii. Face detection dataset. Kaggle dataset, 2025. Accessed: Aug. 22, 2025. 5

[9] Sabri Eyuboglu, Maya Varma, Khaled Saab, Jean-Benoit Delbrouck, Christopher Lee-Messer, Jared Dunnmon, James Zou, and Christopher Ré. Domino: Discovering systematic errors with cross-modal embeddings. *ICLR*, 2022. 1, 2, 5, 6

[10] Sujan Sai Gannamaneni, Rohil Prakash Rao, Michael Mock, Maram Akila, and Stefan Wrobel. Detecting systematic weaknesses in vision models along predefined human-understandable dimensions. *Transactions on Machine Learning Research (TMLR)*, 2025. 1

[11] Andreas Geiger, Philip Lenz, and Raquel Urtasun. Are we ready for autonomous driving? the KITTI vision benchmark suite. In *CVPR*, pages 3354–3361, 2012. 5

[12] Shantanu Ghosh, Rayan Syed, Chenyu Wang, Vaibhav Choudhary, Binxu Li, Clare B. Poynton, Shyam Visweswaran, and Kayhan Batmanghelich. LADDER: Language-driven slice discovery and error rectification in vision classifiers. In *Findings of the Association for Computational Linguistics: ACL*, pages 22935–22970, 2025. 1, 2, 4, 5, 6, 7, 8

[13] Quentin Guimard, Moreno D’Incà, Massimiliano Mancini, and Elisa Ricci. Classifier-to-bias: Toward unsupervised automatic bias detection for visual classifiers. In *CVPR*, pages 15151–15161, 2025. 1, 2

[14] Kaiming He, Georgia Gkioxari, Piotr Dollár, and Ross Girshick. Mask R-CNN. In *ICCV*, pages 2961–2969, 2017. arXiv:1703.06870. 5

[15] Yiyou He, Yaojie Shen, Hongxin Zhang, Pingyu Chen, Lei Ren, and Pin-Yu Liu. Towards non-iid image classification: A dataset and baselines. In *NeurIPS Datasets and Benchmarks Track*, 2021. 3

[16] Saachi Jain, Hannah Lawrence, Ankur Moitra, and Aleksander Madry. Distilling model failures as directions in latent space. In *ArXiv preprint arXiv:2206.14754*, 2022. 2, 5

[17] Younghyun Kim, Sangwoo Mo, Minkyu Kim, Kyungmin Lee, Jaeho Lee, and Jinwoo Shin. Discovering and mitigating visual biases through keyword explanation (bias-to-text). In *CVPR*, 2024. 2, 5

[18] Polina Kirichenko, Pavel Izmailov, and Andrew Gordon Wilson. Last layer re-training is sufficient for robustness to spurious correlations. In *ICLR*, 2023. 8

[19] Zeynep Kuş and Mustafa Aydin. Medsegbench: A comprehensive benchmark for medical image segmentation in diverse data modalities. *Scientific Data*, 11(1):1283, 2024. 3

[20] Sehyun Kwon, Jaeseung Park, Minkyu Kim, Jaewoong Cho, Ernest K. Ryu, and Kangwook Lee. Image clustering conditioned on text criteria. In *ICLR*, 2024. 4

[21] Tsung-Yi Lin, Michael Maire, Serge Belongie, Lubomir Bourdev, Ross Girshick, James Hays, Pietro Perona, Deva Ramanan, C. Lawrence Zitnick, and Piotr Dollár. Microsoft coco: Common objects in context. In *ECCV*, pages 740–755, 2014. 5

[22] Tsung-Yi Lin, Priya Goyal, Ross Girshick, Kaiming He, and Piotr Dollár. Focal loss for dense object detection. *IEEE TPAMI*, 42(2):318–327, 2020. Originally in ICCV 2017 version. 5

[23] Evan Zheran Liu, Aditi Raghunathan, Pang Wei Koh, and Percy Liang. Just train twice: Improving group robustness without training group information. In *Proceedings of the International Conference on Machine Learning (ICML)*, pages 6781–6792, 2021. 3

[24] Ziwei Liu, Ping Luo, Xiaogang Wang, and Xiaoou Tang. Deep learning face attributes in the wild. In *ICCV*, 2015. 3, 5

[25] Yulin Luo, Ruichuan An, Bocheng Zou, Yiming Tang, Jiaming Liu, and Shanghang Zhang. Llm as dataset analyst: Subpopulation structure discovery with large language model. In *ECCV*, pages 235–252. Springer, 2024. 2

[26] Xiaofeng Mao, Yuefeng Chen, Yao Zhu, Da Chen, et al. Coco-o: A benchmark for object detectors under natural distribution shifts. In *ICCV*, 2023. 3

[27] Badr-Eddine Marani, Mohamed Hanini, Nihitha Malaryukil, Stergios Christodoulidis, Maria Vakalopoulou, and Enzo Ferrante. Vig-bias: Visually grounded bias discovery and mitigation. In *ECCV*, pages 414–429. Springer, 2024. 3, 5

[28] Luke Oakden-Rayner, Jared Dunnmon, Gustavo Carneiro, and Christopher Ré. Hidden stratification causes clinically meaningful failures in machine learning for medical imaging. In *Proceedings of the ACM Conference on Health, Inference, and Learning (CHIL)*, pages 151–159, 2020. 1

[29] Shaoqing Ren, Kaiming He, Ross Girshick, and Jian Sun. Faster R-CNN: Towards real-time object detection with region proposal networks. *IEEE TPAMI*, 39(6):1137–1149, 2017. Originally in arXiv:1506.01497 / NIPS 2015 version. 5

[30] Shiori Sagawa, Pang Wei Koh, Tatsunori B. Hashimoto, and Percy Liang. Distributionally robust neural networks. In *ICLR*, 2020. 2, 3, 5, 8

[31] Ignacio Serna, Aytami Morales, Julian Fierrez, and Javier Ortega-Garcia. Sensitiveloss: Improving accuracy and fairness of face representations with discrimination-aware deep learning. In *CVPRW*, pages 0–0, 2020. 3

[32] Laleh Seyyed-Kalantari, Haoran Zhang, Matthew B. A. McDermott, Irene Y. Chen, and Marzyeh Ghassemi. Under-diagnosis bias of artificial intelligence algorithms applied to chest radiographs in under-served patient populations. *Nature Medicine*, 27(12):2176–2182, 2021. 1

[33] Chien-Yao Wang, Alexey Bochkovskiy, and Hong-Yuan Mark Liao. YOLOv7: Trainable bag-of-freebies sets new state-of-the-art for real-time object detectors. In *CVPR*, 2023. 5

[34] Fulton Wang, Julius Adebayo, Sarah Tan, Diego Garcia-Olano, and Narine Kokhlikyan. Error discovery by clustering influence embeddings. In *NeurIPS*, pages 41765–41777, 2023. 2

[35] Michelle Wang and Jia Deng. Towards fairness in visual recognition: Effective strategies for bias mitigation. In *CVPR*, pages 8919–8928, 2020. 3

[36] Xinyuan Yan, Xiwei Xuan, Jorge Piazzentin Ono, Jiajing Guo, Vikram Mohanty, Shekar Arvind Kumar, Liang Gou, Bei Wang, and Liu Ren. Vislix: An XAI framework for validating vision models with slice discovery and analysis. In *Computer Graphics Forum (CGF)*, page e70125, 2025. 1, 3

[37] S. Yenamandra et al. First amplify correlations and then slice to discover bias (facts). In *ICCV*, 2023. 1, 2, 5, 6

[38] Xingxuan Zhang, Yue He, Renzhe Xu, Han Yu, Zheyuan Shen, and Peng Cui. Nico++: Towards better benchmarking for domain generalization. In *CVPR*, pages 16036–16047, 2023. 2, 3, 5

[39] Enshen Zhou, Qi Su, Cheng Chi, Zhizheng Zhang, Zhongyuan Wang, Tiejun Huang, Lu Sheng, and He Wang. Code-as-monitor: Constraint-aware visual programming for reactive and proactive robotic failure detection. In *CVPR*, pages 6919–6929, 2025. 1

SliceLens: Fine-Grained and Grounded Error Slice Discovery for Multi-Instance Vision Tasks

Supplementary Material

A. Prompts

A.1. Prompt Templates Used in SliceLens

This section presents detailed prompt templates used in SliceLens hypothesis generation module.

A.1.1. Knowledge-driven Hypothesis Generation Prompt

The system prompt guides the model to consider various factors, such as object attributes and image quality, and to structure its output in a specific JSON format. This structured output contains task-specific difficulties and attributes that affect model performance. The task-specific difficulties serve as query phrases for slice discovery (the ‘search’ type in the prompt), while the attributes are used for data-driven hypothesis generation (the ‘cluster’ type in the prompt). For specific tasks, task descriptions are provided in user prompts, as detailed in Section A.2. See Figure 8 for details.

A.1.2. Data-driven Hypothesis Generation Prompt

• Grounded Attribute-aware Caption Extraction Prompt.

This prompt directs the model to focus on a specific image region defined by bounding box coordinates and to generate a descriptive caption that highlights potential reasons for failure related to a given attribute. The attribute originates from the “cluster” type prompts discussed in the preceding section. This process is crucial for generating fine-grained, instance-level descriptions from datasets. (See Figure 9 for details).

• Attribute Inference Prompt.

This section outlines a two-step process for inferring attribute values from captions. In the first step, a prompt instructs a Large Language Model (LLM) to extract values or keywords from captions based on given attributes. The second step involves processing the raw list of extracted values or keywords by removing duplicates and irrelevant terms and organizing the remainder into semantically coherent categories. This structured process transforms unstructured outputs from the Vision-Language Model (VLM) into a clean, hierarchical set of attributes and values for subsequent data-driven hypothesis generation. (See Figure 10 for details).

• Refinement Prompt for Grounded Query Phrases .

This prompt instructs the model to convert a structured list of semantic attributes and values into natural language sentences suitable for text-to-image retrieval. The strict constraint to preserve semantics ensures that the resulting

queries accurately reflect the discovered error attributes and values, forming our data-driven hypothesis. (See Figure 11 for details).

A.2. User Prompts for Hypothesis Generation on Specific Datasets

The following user prompts are used as task context to generate hypotheses for the specific tasks or datasets in SliceLens. Each prompt is tailored to the specific characteristics and challenges of its respective dataset.

A.2.1. User Prompt for Waterbirds Dataset

The user prompt for Waterbirds Dataset is as follows:

A model that classifies whether a bird is a water bird or a land bird. The dataset is constructed by cropping out birds from photos and transferring them onto different backgrounds.

A.2.2. User Prompt for CelebA Dataset

The user prompt for CelebA Dataset is as follows:

A model that detects whether a person in an image has blonde hair, considering various attributes of the person.

A.2.3. User Prompt for NICO++ Dataset

The user prompt for NICO++ Dataset is as follows:

A model is used for multi-label classification, classifying images into one of six categories: mammals, birds, plants, airways, waterways, and landways. The dataset consists of real-world images of these categories appearing in six different contexts (dim lighting, outdoor, grass, rock, autumn, and water).

A.2.4. User Prompts for FeSD Dataset

For the FeSD (Fine-grained Error Slice Dataset) experiments, we use two separate prompts: one for detection-related error slices and another for segmentation-related error slices. The user prompt used for object detection hypothesis generation is shown in Figure 12, which focuses on three main error types: false positives, false negatives, and misclassification. Figure 13 shows the comprehensive prompt for instance segmentation tasks, addressing failure modes such as boundary errors, incomplete masks, over-segmentation, and under-segmentation.

These task-specific user prompts enable SliceLens to generate comprehensive failure hypotheses that cover all relevant aspects of detection and instance segmentation models, ensuring thorough coverage of potential error patterns in fine-grained computer vision tasks.

System Prompt for knowledge-driven Hypothesis Generation

You are an expert in computer vision failure analysis. A user will provide a task description (e.g., "a cat body detection"). Your goal is to identify and list all possible reasons why a computer vision model might fail on this task. In your analysis, consider a comprehensive set of factors, including but NOT LIMITED TO:

- Object Attributes
- Background Descriptions
- Image Qualities
- Environmental Conditions
- Limitations in handling edge cases or extreme conditions
- Camera capturing conditions
- Any additional domain-specific challenges

For the given task description, generate a structured and detailed list of failure hypotheses. Your output must include:

- Comprehensive different factors (e.g., Object Attributes, Image Qualities, etc.).
- Under each factor, list comprehensive failure patterns.
- For each failure pattern, include:
 - A title that summarizes the potential failure reason.
 - A description that explains in detail why this might be an issue.
 - A list of prompts to further explore the hypothesis. Each prompt must include:
 - * A prompt field with a specific query or cluster description.
 - * A type field, where the value is either "cluster" or "search". Use "cluster" if the prompt provides a broad description with many possible attributes for further investigation (e.g., "cat colors" or "cat types"). Use "search" if the prompt can be directly used to retrieve relevant images (e.g., "a white cat").
- **IMPORTANT:** Ensure that your final output does not contain any duplicate failure patterns or prompts. Every entry must be unique and directly relevant to image retrieval or image clustering.

Please think through at least three iterations internally to ensure completeness, accuracy, and uniqueness. Then, output your final results in a valid JSON object formatted exactly as follows:

```
1  {
2      "title": "Possible failure reasons for [task description] model",
3      "hypothesis": [
4          "Object Attributes": [
5              {
6                  "title": "[Short title for failure pattern 1]",
7                  "description": "[Detailed explanation]",
8                  "prompts": [
9                      {
10                          "prompt": "[related query or cluster description term]",
11                          "type": "[cluster or search]"
12                      },
13                      ...
14                  ],
15                  ...
16              ],
17              ...
18          ],
19          "Background Descriptions": [ ... ],
20          ...
21      }
22 }
```

Figure 8. The detailed system prompt for generating a comprehensive set of knowledge-driven hypotheses.

A.3. Semantic Relevance Evaluator Prompt

Each algorithm output is processed individually using the following prompt for semantic relevance evaluation:

I have a description of an error pattern from a computer vision model, and a list of ground truth error patterns.

Please identify which of the following ground truth patterns is same with the algorithm output in semantic. For example, Non-upright face (nonvertical pose) is similar to faces with extreme head tilt, but not similar to bicycle lying on ground or bicycle upside down. The ground truth patterns are provided below as a numbered list.

Please respond with ONLY the number of the matching ground truth pattern. If none of the ground truth patterns are a good semantic match, respond with "-1". NOTE: The ground truth patterns and algorithm patterns should indicate the same objects, context, conditions and actions.

Grounded Attribute-aware Caption Extraction

You are an AI model designed to analyze images and provide detailed captions for a specific region relevant to the {Attribute}. The specified region is defined by bounding box coordinates in the format [xmin, ymin, xmax, ymax].

Figure 9. The prompt used to instruct the Vision-Language Model (VLM) for grounded attribute-aware caption extraction. The {Attribute} placeholder is replaced with the specific attribute being analyzed.

Two-Step Prompt for Attribute Inference

Step 1: Attribute Value or Keyword Extraction

You will be given a description of the {Attribute}. Your job is to determine the most relevant {Attribute} based on the provided description. Don't return anything except the result.

Example Input:

Attribute: activity

Caption: The image depicts a person performing a handstand on a purple mat in a spacious, well-lit room with white walls and a high ceiling.

Expected Output:

handstand

If the description is irrelevant to {Attribute}, please output 'none'.

Now, process the provided list:

Step 2: Keyword Refinement and Clustering

You are a helpful text clustering assistant. You will be given a list of keyword text. Your job is to refine and categorize the list to clusters. Your goal is to process the provided keyword list to:

- **Eliminate Duplicate Semantics:** Identify and remove keywords that represent similar meaning, even if expressed differently (e.g., 'car' and 'automobile').
- **Eliminate irrelevant keywords:** Identify and remove keywords that are not related to {Attribute}.
- **Group into Categories:** Organize keywords into distinct, non-overlapping categories based on their meaning and context.
- **Ensure Clarity:** Avoid overly broad or overly narrow categories. Each keyword should fit logically within its assigned category.

Example Input:

['car', 'automobile', 'vehicle', 'bike', 'bicycle', 'motorcycle', 'transport']

Expected Output (JSON format):

{ "transport": ["car", "bike", "motorcycle"] }

Please think and improve your results at least four turns. And then eliminate duplicate semantics in one more turn. Now, process the provided keyword list and output the final results in JSON format at the end with unique, non-overlapping semantics.

Figure 10. The prompts used for attribute inference via text clustering. Step 1 extracts relevant values from attributes and captions, and Step 2 clusters them into semantic categories. The {Attribute} placeholders are replaced with the specific task context and attribute being analyzed.

B. More Detailed Experimental Results

B.1. LLMs and VLMs Selection in SliceLens

We compare different LLMs for generating slice hypotheses: Gemini-2.5-Pro (our choice), GPT-4o, and Claude-3.5-Sonnet. Performance variations are minimal (0.69 vs. 0.68 vs. 0.67 on NICO++ (95%)), suggesting that the hypothesis generation method is robust to LLM choice. This robustness also indicates that the world knowledge of powerful LLM in vision tasks is sufficient for analyzing task-intrinsic

difficulties and data distribution attributes.

We evaluated three different Vision-Language Models (VLMs) for slice confidence estimation to analyze the trade-off between effectiveness and computational efficiency. As shown in Table 5, our evaluation on the NICO++ (95%) dataset reveals a clear distinction between model families.

Embedding-based models like SigLIP are exceptionally fast due to their use of pre-computed embeddings, but they achieve lower precision as their global representations struggle with fine-grained discrimination. In contrast,

Refinement Prompt for Grounded Query Phrases

You will be given a JSON list of attributes with values or cluster names with categories. These cluster names are summarized from descriptions related to the `{Attribute}`. Your job is to compose a text to image retrieval prompt from each category and item in the list. The prompt should be phrases or sentences not keywords and only contain the given information.

You can start or end with general descriptions, for example “a photo of” etc. Please DO NOT add or modify the context and semantics. The output JSON format is:

```
1 {"results": [prompt1, prompt2, ...]}
```

Now process the list and generate prompts one by one for each items.

Figure 11. The prompt used for refining attributes and values into grounded query phrases. The `{Attribute}` placeholder is replaced with the specific task context and attribute being analyzed.

User Prompt for FeSD Object Detection Hypothesis Generation

An object detection model designed to detect `{label}`. Specifically, consider and describe possible scenarios for the following types of errors:

False Positive: In what situations might other objects be mistakenly detected as `{label}`?

False Negative: In what situations might `{label}` fail to be detected by the model?

Misclassification: In what situations might `{label}` be incorrectly detected as another object class?

Figure 12. The specialized user prompt used for object detection hypothesis generation on the FeSD dataset. The prompt focuses on the three main types of detection errors: false positives, false negatives, and misclassification. The `{label}` placeholder is replaced with the specific object class being analyzed.

Table 5. Comparison of different VLMs for slice confidence estimation on NICO++ (95%). GPT-4o tested with 10 concurrent requests. CLIP/SigLIP times exclude embedding extraction overhead.

VLM	Precision@10	Speed
SigLIP	0.51	0.1 s /1000 images
GPT-4o	0.71	5 min /1000 images
Qwen-2.5-VL-7B	0.69	10 s /1000 images

reasoning-based models demonstrate superior performance. While GPT-4o achieves the highest precision@10 (0.71), its API latency is prohibitive at 5 minutes per 1,000 images.

Qwen-2.5-VL-7B, deployed locally with the VLLM framework, offers the best practical balance. To optimize its performance, we structure the prompts to share the same system prompt and image prefix. Leveraging prefilling technology, only the text in the user prompts requires processing after the initial slice confidence computation. Furthermore, the model’s output is restricted to “yes” or “no”, which makes the decoding process highly efficient. As a result, it delivers competitive precision (0.69) with a significantly lower latency of 10 seconds per 1,000 images on one

A100 GPU. This makes it our choice for SliceLens.

B.2. HiBug Baseline Implementation Details

For a fair comparison with HiBug on our FeSD dataset, we generated a comprehensive attribute corpus following the HiBug methodology. We generated visual attributes relevant to object detection failures by interactively chatting with ChatGPT. Table 6 presents the complete set of attributes used for HiBug’s instance-level analysis on detection tasks.

This comprehensive attribute set demonstrates HiBug’s systematic approach to instance-level analysis through pre-defined visual attributes. Each attribute is designed to capture specific visual characteristics that may contribute to model failures.

B.3. Model Improvement Experiment Setup Details

B.3.1. Model Improvement on Image Classification

We evaluate the actionability of discovered slices via model repair experiments on CelebA and Waterbirds, following the official Ladder implementation. We use the pre-trained ResNet weights and the author-released discovered slices provided by Ladder, and modify only the final error-mitigation stage in the official training scripts for CelebA

User Prompt for FeSD Instance Segmentation Hypothesis Generation

An Instance Segmentation model designed to detect and segment `{label}`. Think systematically from the following perspectives, and describe possible scenarios for each type of error below:

False Positive: In what situations might other objects be mistakenly segmented as `{label}`?

False Negative: In what situations might `{label}` fail to be segmented?

Misclassification: In what situations might `{label}` be incorrectly segmented as another object class?

Boundary Error: When might the segmentation mask boundary deviate from the true object contour (e.g., occlusion, uneven lighting, blurry edges)?

Incomplete Mask: When might the model segment only part of the `{label}` instead of the entire object?

Over-segmentation: When might the model mistakenly split one `{label}` instance into multiple segments?

Under-segmentation: When might the model merge multiple nearby `{label}` instances into a single mask?

Figure 13. The specialized user prompt used for instance segmentation hypothesis generation on the FeSD dataset. This prompt addresses comprehensive errors (false positives, false negatives, misclassification, boundary errors, incomplete masks, over-segmentation, under-segmentation) to cover potential failure patterns thoroughly in instance segmentation tasks. The `{label}` placeholder is replaced with the specific object class being analyzed.

and Waterbirds. For Ladder, we follow its original repair procedure: each discovered slice defines a similarity score over validation samples. For every slice, we fine-tune a separate classifier using the top and bottom n samples by similarity and aggregate predictions via Ladder’s ensemble.

For Facts, Domino, and SliceLens, the discovered slices exist only within local subsets, often containing fewer samples than required by Ladder’s per-slice training. Thus, we adopt the unified Discriminative Fine-tuning for Repair (DFR) framework, which serves as the underlying procedure used in Ladder. For each sample, we compute a single confidence score by taking the maximum across all discovered slices, representing the likelihood of any failure pattern.

Fine-tuning is applied only to the classifier head on the top and bottom subsets ranked by this score, producing a single repaired classifier without ensemble aggregation. All hyperparameters match the official Ladder scripts except that we randomize the random seed for each run to compute standard deviations while the original Ladder implementation uses a fixed seed.

B.3.2. Object Detection Model Improvement on Fine-Grained Patterns

We use the COCO bicycle subset (3,252 images, 7,113 *bicycle instances*) and a pretrained Faster R-CNN (ResNet-50-FPN) model. The baseline repair method is fine-tuning on all COCO images containing at least one bicycle instance. Optimization uses SGD (momentum 0.9), weight decay 5×10^{-4} , batch size 16, initial learning rate 1×10^{-5} , and a MultiStepLR scheduler with milestones at epochs 8 and 11 ($\gamma=0.1$) for a total of 10 epochs.

Confidence scores of instances for the validated error slice “*bicycle partially occluded by a person*” are computed by SliceLens slice discovery method. The image-level bi-

nary attribute is defined as $\mathbf{1}\{\max_{\text{instances}} s_i \geq 0.9\}$, where s_i is the instance confidence score. Each object class defines a *group* (e.g., person, bicycle). For example, a pair (person, True) denotes a person instance co-occurring with a likely “*bicycle partially occluded by a person*” case, whereas (bicycle, False) represents a bicycle instance with no such occlusion in the same image. We initialize weights uniformly across all (group, attribute) pairs. Only detection-head losses (classification and box regression) are reweighted; RPN losses (objectness, RPN box) remain unweighted and are added directly to the total loss.

For the grounded repair, we adapt the online GroupDRO framework to instance-level objectives. Per-group losses are computed by aggregating proposal-level classification and regression losses within each group. The weighted detection-head loss is then

$$\tilde{\mathcal{L}}_{\text{head}} = \frac{\sum_u q_u \mathcal{L}_u}{\sum_u q_u},$$

where \mathcal{L}_u is the mean detection loss for group u and q_u is its current weight. The total loss adds unweighted RPN terms:

$$\mathcal{L}_{\text{total}} = \tilde{\mathcal{L}}_{\text{head}} + \mathcal{L}_{\text{RPN,obj}} + \mathcal{L}_{\text{RPN,box}},$$

where $\mathcal{L}_{\text{RPN,obj}}$ and $\mathcal{L}_{\text{RPN,box}}$ are the RPN objectness and bounding box regression losses, respectively.

After each iteration, group weights are updated online as

$$q_u \leftarrow q_u \exp(\eta \mathcal{L}_u), \quad q_u \leftarrow q_u / \sum_v q_v,$$

with $\eta=10^{-5}$. The GroupDRO variant uses batch size 16, learning rate 5×10^{-5} , and the same optimizer settings and scheduler as the baseline.

In summary, each iteration aggregates instance losses by group, computes a reweighted detection-head loss, adds

RPN losses, and updates the group weights using the exponential rule above. Uniform weight initialization is applied at the start of fine-tuning, and all other architectural details follow the main text.

B.4. SliceLens Results on FeSD Dataset

B.4.1. Detailed Object Detection Results on FeSD Dataset

Table 7 provides comprehensive Precision@10 results for all 21 ground truth error slices in the object detection setting, complementing the summary results presented in the main paper. SliceLens achieves an overall average Precision@10 of 0.729, with 5 perfect matches and valid predictions for all ground truth slices.

The detailed results reveal SliceLens’ effectiveness across both false positive and false negative error types. The method demonstrates particularly strong performance on systematic failure patterns such as “Red traffic sign is mistakenly detected as stop sign” and “Artistic face is mistakenly detected as face” achieving perfect Precision@10 scores. Even for challenging cases like “Nonvertical face in the image missed”, SliceLens maintains competitive performance with Precision@10 scores of 0.8.

B.4.2. Instance Segmentation Results on FeSD Dataset

To demonstrate the generalizability of SliceLens beyond object detection, we evaluate our method on instance segmentation tasks using the FeSD dataset.

Table 8 presents the detailed Precision@10 results for all 21 ground truth error slices in the instance segmentation setting. SliceLens achieves an overall average Precision@10 of 0.805, demonstrating strong performance across diverse segmentation failure patterns. The method successfully identifies 8 perfect matches (Precision@10 = 1.0) and achieves valid matches for 20 out of 21 ground truth slices.

The results demonstrate that SliceLens effectively transfers to instance segmentation tasks, maintaining high precision across various failure modes including occlusion patterns, object state variations, and contextual confusion scenarios. Notably, the method achieves perfect precision on challenging slices such as “laptop keyboard merged with laptop body” (fine-grained object parts), “Tie boundary unclear due to color blending” (visual similarity challenges), and shape-related patterns like “Sliced orange under-segmented due to shape change”. The method shows robust performance across different object categories including fruits, furniture, and everyday objects, with only one slice: “Surfboard on land missed (expected water context)” receiving zero precision, indicating the challenge of detecting surfboards in land-based contexts.

C. Error Slice Discovery Tool based on SliceLens

To demonstrate the practical utility of SliceLens, we developed a production-ready tool for error slice discovery in computer vision systems. While the SliceLens described in our paper is an automated pipeline given a task context for evaluation purposes, the deployed tool is designed for an interactive workflow. It provides a user interface that allows human expertise to be incorporated into each stage of the discovery process. The following screenshots illustrate the key components of our implementation across different steps.

C.1. Interactive Chat Interface for Hypothesis Generation

Figure 14 shows the main interface of the tool, featuring a dual-panel design with a data gallery on the left for dataset visualization and an interactive chatbox on the right for conversational hypothesis generation and data retrieval.

C.2. Hypothesis Selection and Submission

Figure 15 demonstrates the hypothesis selection interface, where users can review LLM-generated failure pattern hypotheses and select the most promising candidates for validation. The interface allows users to submit selected hypotheses for automated slice discovery and trend analysis.

C.3. Hypothesis Verification Task Management

Figure 16 presents the task management interface, which displays all submitted hypotheses along with their validation status. Each hypothesis-validation task runs asynchronously, allowing users to monitor progress and access results upon completion. These tasks are executed in batches to improve performance through prefilling and batched request optimization in the VLLM framework.

C.4. Error Slice Identification Results

Figure 17 shows an example of the slope trend analysis results for a validated hypothesis. The interface presents the statistical relationship between slice confidence scores and accuracy. Unlike SliceLens in the paper, which reports error rates, the tool supports analysis using either accuracy or error rate, and the slope trend analysis adapts automatically to the selected metric. This provides robust evidence supporting the validity of the discovered error slices across multiple metrics.

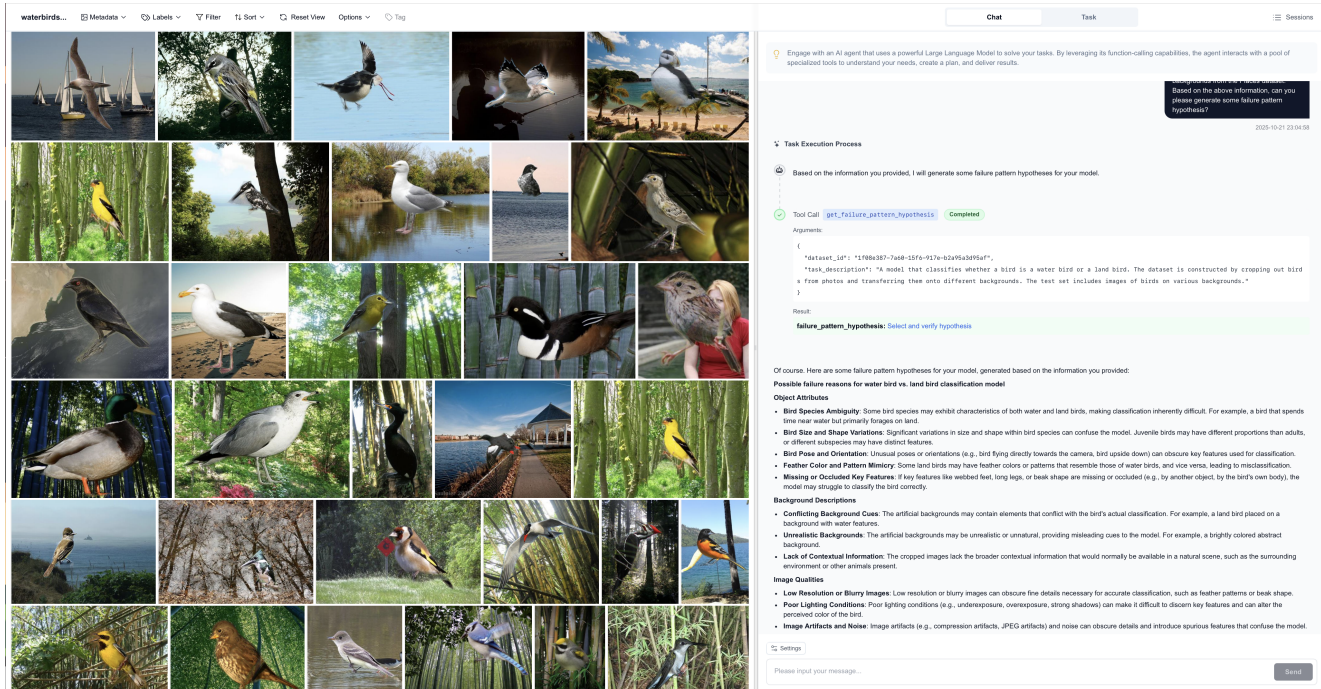


Figure 14. **SliceLens main interface with interactive chat functionality.** The left panel displays the data gallery for dataset visualization, while the right panel provides a conversational interface for users to interact with the LLM for hypothesis generation and error slice discovery tasks.

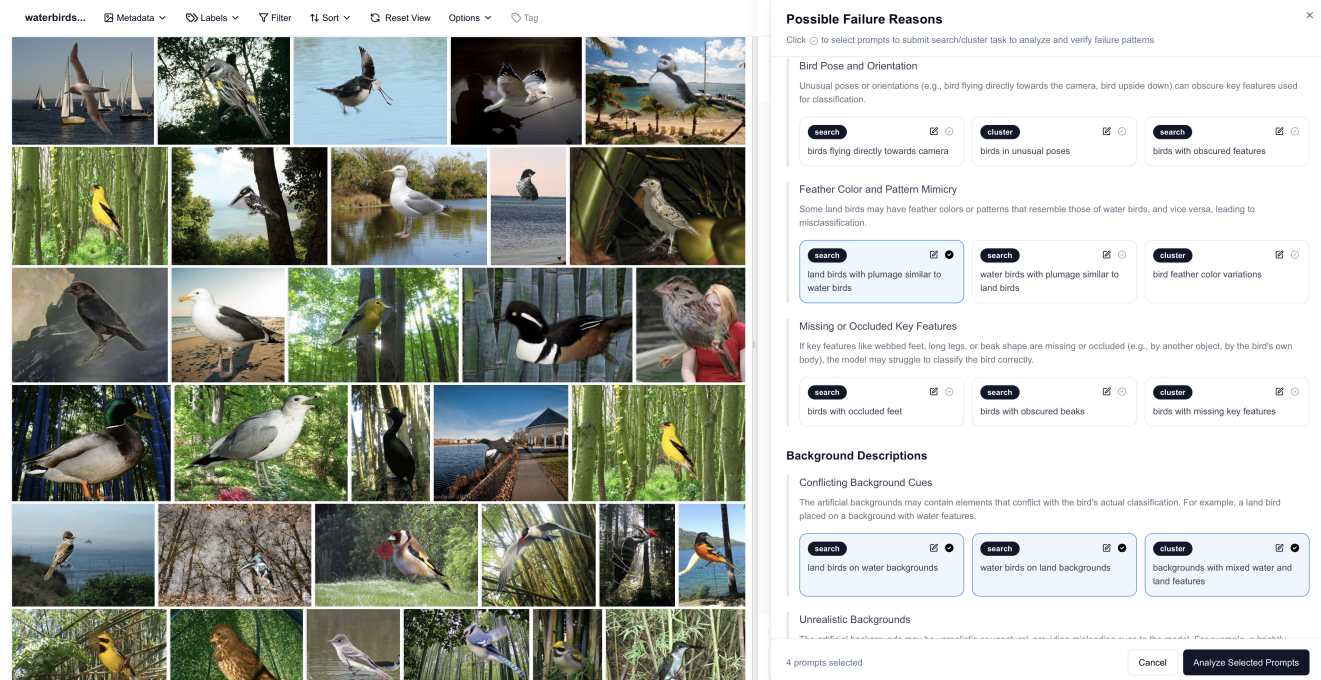


Figure 15. **Hypothesis selection and submission interface.** Users can review automatically generated failure pattern hypotheses, assess their plausibility, and submit selected candidates for validation.

Table 6. HiBug attribute corpus generated for instance-level error slice discovery on FeSD dataset. Attributes are generated using ChatGPT following HiBug methodology. Each attribute includes categorical values, prompt templates, and evaluation questions for systematic analysis.

Attribute	Type	Values	Prompt Template	Evaluation Question
Object Reality	Description	real_object, image_in.image, artistic_rendering, reflection_mirror, screen_display	A detected object in object reality	What is the object in the photo, and is it a true representation of reality?
Image Sharpness	Description	very_sharp, sharp, slightly_blurry, very_blurry	A detected object with sharp image_sharpness	How would you rate the sharpness of the detected object in the photo?
Object Visibility	Description	100_percent, 50_percent, less_than_20	80_percent, 30_percent, A detected object with 90% object visibility	What is the object_visibility_percentage of the detected object in the photo?
Vehicle Subtype	Description	car, truck, bus, trailer, van, motorcycle, bicycle, stroller, cart, dumpster	A detected car with a SUV subtype	What is the vehicle_subtype of the detected object in the photo?
Person Activity	Description	standing, walking, sitting, riding_bicycle, in_vehicle, running, lying	A #DETECTED_OBJECT doing #1	What is the activity of the person in the photo?
Face Age Group	Description	infant, child, teenager, young_adult, adult, elderly	A #LABEL in the youth #1	What age group does the detected object's face belong to in the photo?
Face Orientation	Description	upright_frontal, upright_side, tilted, horizontal, upside_down	A #LABEL with #1 face_orientation	What is the orientation of the face in the detected object in the photo?
Object State	Description	closed, partially_open, fully_open, in_use, idle	A #LABEL in motion	What is the object_state of the detected object in the photo?
Object Material	Description	solid, paper, metal, glass, plastic, fabric	A #1 ball with metal material	What material is the detected object in the photo made of?
Object Scale	Description	fills_frame, dominates, medium, small, tiny	A detected object with a small object scale in the frame	What is the object_scale_in_frame of the detected object in this photo?
Object Size	Description	small, medium, large	A #LABEL with small object_size	What is the size of the detected object in the photo?
Occlusion Level	Description	not_occluded, partially_occluded, fully_occluded	par-heav- A detected object with low occlusion level	What is the occlusion level of the detected object in the photo?
Motion Blur	Binary	yes, no	-	Is the detected object in the photo showing signs of motion blur?
Lighting Condition	Description	bright, normal, dark	An #LABEL in #1 lighting condition	What is the lighting condition of the detected object in the photo?
View Angle	Description	frontal, side, back, top	A #LABEL from a #1 view angle	What is the view angle of the detected object in the photo?
Object Truncation	Description	complete, partially_truncated, heavily_truncated	A truncated detected object	What is the object_truncation value of the detected object in the photo?
Color Contrast	Description	low_contrast, medium_contrast, high_contrast	A #LABEL with high color contrast	What is the color contrast of the detected object in the photo?
Background Clutter	Description	simple_background, moderate_clutter, heavy_clutter	A #LABEL with busy background_clutter	What is the background clutter of the detected object in the photo?
Object Distance	Description	close, medium, far	A detected object at close distance	What is the distance of the detected object in the photo?
Object Pose	Description	upright, tilted, horizontal, inverted	An #LABEL in a #1 pose	What is the pose of the detected object in the photo?
Mirror/Glass Presence	Binary	yes, no	-	Is there a mirror or glass present in the photo?
Color Similarity	Description	distinct, similar_to_background, blends_with_background	simi- A #LABEL with #1 ob- ject_color_similarity	What is the similarity between the detected object and the color of the photo?
Object Reflection	Description	no_reflection, slight_reflection, strong_reflection	A detected object with a shiny reflection	What does the detected object in the photo reflect?
Time of Day	Description	morning, noon, afternoon, evening, night	A sky with morning light	What is the time of day of the detected object in the photo?
Texture Pattern	Description	smooth, textured, patterned	A #LABEL with #1 texture pattern	What is the texture pattern of the detected object in the photo?
Partial Visibility	Binary	yes, no	-	Is the detected object in the photo partially visible?

Table 7. **Detailed Object Detection Results on FeSD Dataset.** Complete Precision@10 scores for each ground truth error slice, showing the breakdown of SliceLens performance across different failure types (FP: False Positive, FN: False Negative).

GT ID	GT Slice Name	GT Size	Best Predicted Slice	P@10
0	Stroller trolley is mistakenly detected as a bicycle	31	folding bicycle	0.2
1	Blurry face missed	825	faces with motion blur	0.5
2	Cars that are partially obscured missed.	1003	Car that are more than 30% obscured	0.8
3	Nonphysical face(e.g., face reflected in a mirror) is mistakenly detected as face	457	Faces on screens: a face appearing on a TV, computer monitor, or phone within the image.	0.7
4	Paper is mistakenly detected as book	151	Notebooks, journals, or planners that look like a book	0.5
5	Red traffic sign is mistakenly detected as stop sign	1611	red octagonal object near stop sign	1.0
6	Person in the car missed	162	out of focus person	0.9
7	Closed umbrella missed	24	Closed umbrella	0.6
8	Artistic face is mistakenly detected as face	501	Statues, busts, or sculptures	1.0
9	Partial face missed	1058	faces partially hidden by objects	0.8
10	Vase with no flower or plants inside missed	46	Vase with no flower or plants inside	0.5
11	Baby face missed	101	baby faces	1.0
12	Trailer is mistakenly detected as truck	230	Trailers that look like a truck	0.7
13	Dumpster is mistakenly detected as truck	275	Dumpsters or large bins that look like a truck	1.0
14	Artificial face is mistakenly detected as face	182	objects resembling faces	0.4
15	Open book missed	26	an open book	0.9
16	Watch missed when detecting clock	22	watch that looks like a clock	1.0
17	Open suitcase missed	11	suitcase that will not close	0.8
18	Bicycles seen from the front/back that being ridden/pushed by people	303	bicycle partially occluded by a person	0.8
19	Cars with open doors are mistakenly detected as truck	125	Freight cars that look like a truck	0.4
20	Nonvertical face in the image missed	35	faces with extreme head tilt	0.8
Average Precision@10				0.729
Perfect Matches (P@10 = 1.0)				6/21
Valid Matches (P@10 > 0)				21/21

Table 8. **Detailed Instance Segmentation Results on FeSD Dataset.** Precision@10 scores for each ground truth error slice, showing SliceLens' performance across diverse segmentation failure patterns.

GT ID	GT Slice Name	GT Size	Best Predicted Slice	P@10
0	Clustered bananas merged, boundaries unclear	183	banana bunch	0.8
1	Airplane boundary expanded under occlusion	25	airplanes with custom paint jobs	0.9
2	Bed over-segmented with pet	36	pet lying on bed	0.9
3	Laptop keyboard merged with laptop body	136	laptop keyboard	1.0
4	Paper mis-segmented as book	334	Notebooks, journals, or planners that look like a book	0.7
5	Apple logo mis-segmented as apple	34	partially occluded apple	0.7
6	Tie boundary unclear due to color blending	82	ties similar to other clothing	1.0
7	Sliced carrot under-segmented due to shape change	432	bunches of carrots	0.9
8	Adjacent toys merged with teddy bear	81	teddy bear with accessories	1.0
9	Clustered oranges merged, boundaries unclear	37	pile of oranges	0.7
10	Open suitcase missed (non-canonical form)	12	overstuffed and bulging suitcase	0.6
11	Open book missed due to shape variation	29	open book	0.6
12	Clustered apples merged, boundaries unclear	45	apple in fruit stand	1.0
13	Sliced banana under-segmented due to shape change	90	Banana slice	0.7
14	Closed umbrella missed (non-typical pose)	78	Closed umbrella	1.0
15	Vase without flowers missed due to context prior	136	Vase with no flowers or plants inside	0.6
16	Sliced orange under-segmented due to shape change	97	orange slice	1.0
17	Bed over-segmented together with person	44	person lying on bed	1.0
18	Surfboard on land missed (expected water context)	36	-	0.0
19	Watch missed when segmenting clock	25	watch that looks like a clock	1.0
20	Sliced apple under-segmented due to shape change	82	apple slice	0.8
Average Precision@10				0.805
Perfect Matches (P@10 = 1.0)				8/21
Valid Matches (P@10 > 0)				20/21

waterbirds...
Metadata
Labels
Filter
Sort
Reset View
Options
Tag

Chat
Task

0.9961 waterbird_det/accuracy: false

0.996 waterbird_det/accuracy: false

0.9949 waterbird_det/accuracy: false

0.9946 waterbird_det/accuracy: false

0.9939 waterbird_det/accuracy: false

0.9928 waterbird_det/accuracy: false

0.9923 waterbird_det/accuracy: false

0.9919 waterbird_det/accuracy: false

0.9909 waterbird_det/accuracy: false

0.9905 waterbird_det/accuracy: false

0.9899 waterbird_det/accuracy: false

0.9887 waterbird_det/accuracy: false

0.9885 waterbird_det/accuracy: false

0.9882 waterbird_det/accuracy: false

0.9868 waterbird_det/accuracy: false

0.9862 waterbird_det/accuracy: false

0.9858 waterbird_det/accuracy: false

0.9846 waterbird_det/accuracy: false

0.9839 waterbird_det/accuracy: false

0.9838 waterbird_det/accuracy: false

0.9834 waterbird_det/accuracy: false

0.9815 waterbird_det/accuracy: false

💡 For complex, multi-step tasks that require a structured approach, you can use a predefined tasks in Task tab. These tasks are designed to handle specific, high-value scenarios where a fixed process is more reliable than an open-ended chat. Simply choose a workflow, fill out the required parameters, and the system will execute the task for you.

Task List

Instructions:

1. Create tasks with your prompt.
2. Select multiple tasks and click "Run Selected".

Run Selected New Task

Q Data Search & Analysis complete
Prompt: water birds on land backgrounds
21/10/2025, 23:10 | Bolt

Q Data Search & Analysis complete
Prompt: land birds on water backgrounds
21/10/2025, 23:10 | Bolt

Q Data Search & Analysis complete
Prompt: Birds in snowy conditions
15/9/2025, 02:13 | Bolt

Q Data Search & Analysis complete
Prompt: Birds in rainy conditions
15/9/2025, 02:13 | Bolt

Q Data Search & Analysis complete
Prompt: Birds in foggy conditions
15/9/2025, 02:13 | Bolt

Q Text-Conditioned Clustering complete
Prompt: Background dominance in bird images
15/9/2025, 02:13 | Bolt

Q Data Search & Analysis complete

Figure 16. **Error slice verification task management interface.** The interface displays all submitted validation tasks with their current status, allowing users to track progress and access completed results including discovered slice data and trend analysis.

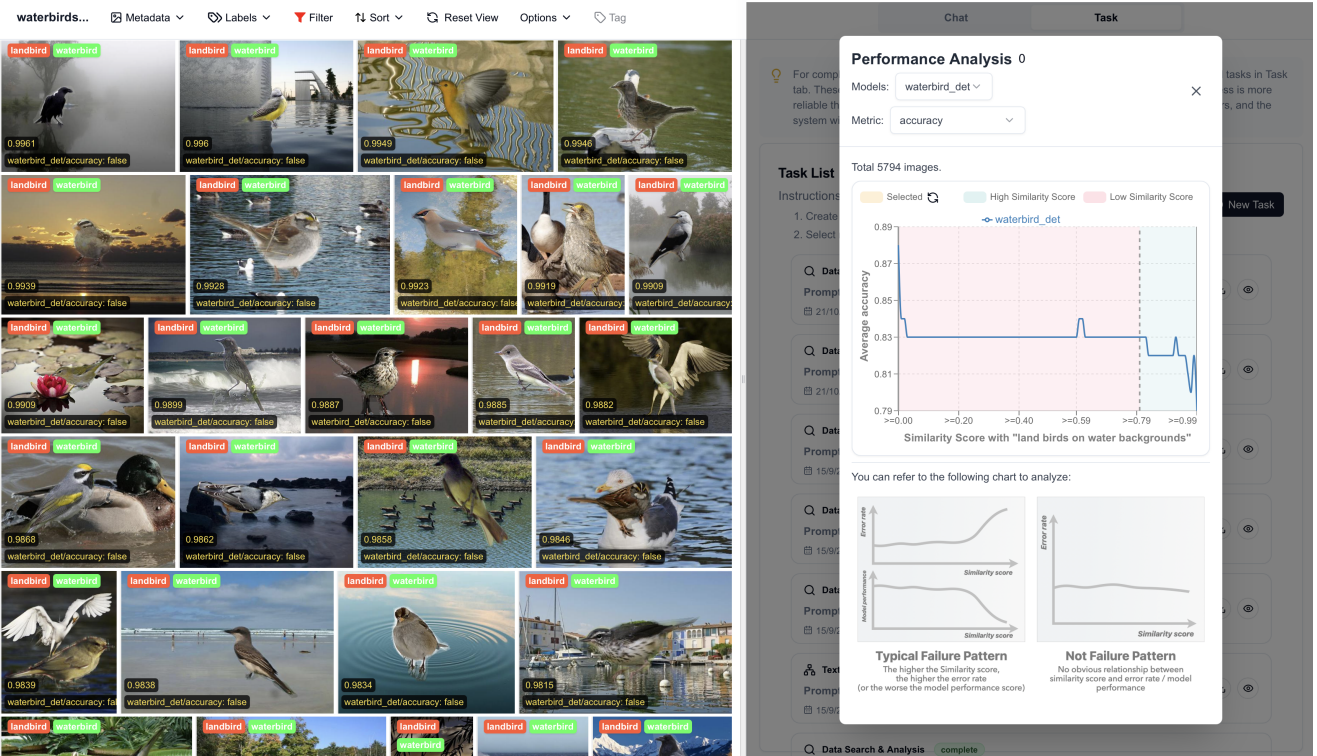


Figure 17. **Trend analysis results interface.** Example showing the statistical validation of a hypothesis through slope trend analysis between slice confidence scores and model performance, demonstrating robust evidence for discovered error slices. Note that the Y-axis in this example is *model accuracy*, not *model error rate*; therefore, a downward trend(rather than a upward trend) of the curve suggests it is a failure pattern.